ResearchGate

See discussions, stats, and author profiles for this publication at: https://www.researchgate.net/publication/221712827

Molecular Description of Indigo Oxidation Mechanisms Initiated by OH and OOH Radicals

ARTICLE *in* THE JOURNAL OF PHYSICAL CHEMISTRY A · MARCH 2012

Impact Factor: 2.69 · DOI: 10.1021/jp211493k · Source: PubMed

CITATIONS
4

READS
80

4 AUTHORS, INCLUDING:

Cristina Iuga
Metropolitan Autonomous University
43 PUBLICATIONS **342** CITATIONS
SEE PROFILE

Juan Raul Alvarez-Idaboy
Universidad Nacional Autónoma de México
121 PUBLICATIONS **2,177** CITATIONS
SEE PROFILE

Available from: Cristina Iuga
Retrieved on: 26 January 2016

THE JOURNAL OF PHYSICAL CHEMISTRY A

Article

pubs.acs.org/JPCA

Molecular Description of Indigo Oxidation Mechanisms Initiated by OH and OOH Radicals

Cristina Iuga,*[,†] Elba Ortíz,[†] J. Raul Alvarez-Idaboy,[‡] and Annik Vivier-Bunge[§]

[†]Departamento de Ciencias Básicas, Universidad Autónoma Metropolitana-Azcapotzalco, Av. San Pablo 180, México D.F. 02200, México

[‡]Departamento de Física y Química Teórica, Facultad de Química, Universidad Nacional Autónoma de México, México D.F. 04510, México

[§]Departamento de Química, Universidad Autónoma Metropolitana-Iztapalapa, Av. San Rafael Atlixco 186, México D.F. 09340, México

Supporting Information

ABSTRACT: In this work, we report a quantum chemistry mechanistic study of the hydroxyl (•OH) and hydroperoxyl (•OOH) radicals initiated oxidation of indigo, within the density functional theory framework. All possible hydrogen abstraction and radical addition reaction pathways have been considered. We find that the reaction between a free indigo molecule and an •OH radical occurs mainly through two competing mechanisms: H-abstraction from an NH site and •OH addition to the central C═C double bond. Although the latter is favored, both channels occur, the indigo chromophore group structure is modified, and thus the color is changed. This mechanism adequately accounts for the loss of chromophore in urban air, including indoor air such as in museums and in urban areas. Regarding the reactivity of indigo toward •OOH radicals, only •OOH-addition to the central double bond is thermodynamically feasible. The corresponding transition state free energy value is about 10 kcal/mol larger than the one for the •OH initiated oxidation. Therefore, even considering that the •OOH concentration is considerably larger than the one of •OH, this reaction is not expected to contribute significantly to indigo oxidation under atmospheric conditions.

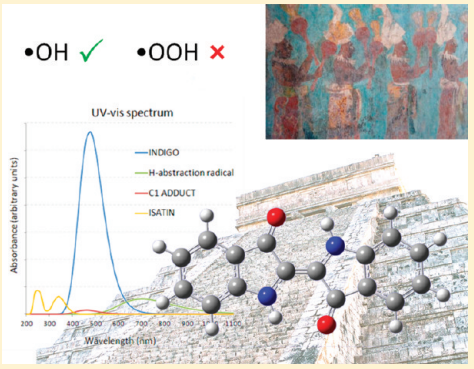

INTRODUCTION

An important issue connected with the chemistry of artwork conservation involves the understanding, at the molecular level, of the degradation mechanisms of dyes. Fading of colored fibers affects the appearance and mechanical properties of textile objects; thus, the comprehension of photo-oxidation chemical pathways and fading mechanisms is needed to develop proper preventive conservation strategies.[1]

Indigo is a blue dye that has been widely used for thousands of years as a pigmenting agent. It is one of the most light-stable organic dyes, a characteristic that explains its longevity as a colorant.[2] It deteriorates slowly with the passing of time under the effect of light, humidity, and oxidizing agents. As a result, the blue colored material changes into colorless products. The recent introduction of ozone and other anthropogenic pollutants into urban air may cause the fading and degradation of dyes and other components of paintings.

Studies on the fading of indigo performed more than 80 years ago report that indigo is photo-oxidized by a very large number of substances rich in oxygen, yielding mainly a yellow product called isatine.[3] Grosjean et al.[4−6] described the fading of several dyes after being exposed to high ozone concentration in the dark. More recently, Novotna and co-workers[7] studied the degradation of indigo in a dichloromethane solution and showed that isatin was the major degradation product. In fact, isatin[8] (1*H*-indole-2,3-dione) was first discovered by Erdmann and Laurent in 1840 as a product arising from the oxidation of indigo using nitric and chromic acids.

The chemistry of the fading of indigo on textiles is a topic that has received only limited attention in the conservation literature since its fading is not often noticeable. However, the degradation of indigo on cotton is important in the textile industry, especially as it relates to indigo-dyed blue jeans.[7] The demand for blue jeans that have been selectively faded resulted in the development of an oxidative process known as acid-washing. However, after treatment, the denim tends to yellow due to the degradation of indigo to yield isatin and anthranilic acid.[9,10]

No molecular study of the reaction mechanism of indigo with oxygen radical species in general has been published. Yet, it is well-known that the oxidative transformation of organic compounds in the troposphere is driven mainly by •OH free radicals. These reactions commonly fall into two basic types of mechanisms, i.e., addition to an aromatic ring or unsaturated bond (hydroxylation) and abstraction of a hydrogen atom.[11]

Received: November 29, 2011
Revised: March 8, 2012
Published: March 18, 2012

ACS Publications © 2012 American Chemical Society

Peroxyl radicals also play a central role in the chemistry of the troposphere. $\bullet HO_2$ is the simplest peroxyl radical and the one found in the largest concentration in the atmosphere (peak concentrations range between 10^8 and 10^9 molecules cm^{-3}). Organic peroxyl radicals ($\bullet RO_2$, where R is a carbon-containing chain) are generated in the atmospheric oxidation of biogenic and anthropogenic VOCs. These peroxyl radicals are intimately connected to various tropospheric chemical cycles through reactions involving the radical families $\bullet HOx$ ($\bullet OH + \bullet HO_2$) and $\bullet NOx$ ($\bullet NO + \bullet NO_2$). By oxidizing $\bullet NO$ to $\bullet NO_2$, $\bullet RO_2$ are key reactants in the photochemical production of tropospheric ozone.

Moreover, $\bullet RO_2$ may react directly with organic molecules, mainly in polluted atmospheres, in which the ratio between $\bullet HO_2$ and $\bullet OH$ radicals is high.[12] Hermans et al.[13] have shown that reaction of $\bullet HO_2$ with formaldehyde, acetone, and other carbonyl compounds significantly influence the $\bullet HOx$ budget at low temperatures.

The indigo stability has been studied by both experimental and theoretical methods.[14] In particular, it has recently been investigated by Yamazaki et al.[15] using quantum chemistry methods. The authors find that the exceptional photostability of indigo is the result of rapid internal conversion via intramolecular single-proton transfer, combined with a high barrier for trans → cis isomerization.

The molecular mechanism of indigo fading under oxidative conditions has not been studied. Many individual channels have to be considered, in principle, and it is not possible to study all of them experimentally. Thus, computational studies constitute an essential tool. In this work, we have carried out a detailed mechanistic study on the hydroxyl ($\bullet OH$) and hydroperoxyl ($\bullet OOH$) radicals-initiated oxidation of indigo dye, in the gas phase. All possible reaction pathways have been considered.

COMPUTATIONAL METHODOLOGY

All electronic calculations were performed with the Gaussian 09 package.[16] Geometry optimizations and frequency calculations have been carried out using the M05−2X functional[17] in conjunction with the 6-311++G(d,p) basis set. The M05-2X functional has been recommended for kinetic calculations by its developers, and it has been also successfully used by independent authors for that purpose.[18−31] Unrestricted calculations were used for open shell systems. Local minima and transition states were identified by the number of imaginary frequencies: local minima have only real frequencies, while transition states are characterized by the presence of a single imaginary frequency that corresponds to the expected motion along the reaction coordinate. Relative energies are calculated with respect to the sum of the separated reactants. Zero-point energies (ZPE) and thermal corrections to the energy (TCE) are included in the determination of energy barriers.

We have assumed that reactions take place according to the complex two-step mechanism typical of radical-molecule reactions,[32] in which the initial step leads to the formation of a prereactive complex that is in equilibrium with the reactants, and the second step is the irreversible formation of the products. The prereactive complexes and the transition structures are designated by the acronyms RC and TS, respectively.

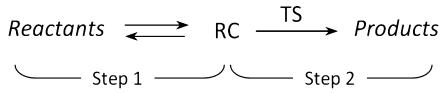

Branching ratios have been calculated at temperature T according to the following expression, which yields the amount of product i

$$\%_i = \frac{w_i e^{-\Delta G^{\ddagger}_i/RT}}{\sum_i w_i e^{-\Delta G^{\ddagger}_i/RT}} \quad (1)$$

where $\Delta G^{\ddagger}_i$ is the Gibbs free energy barrier of each channel and w_i is the degeneracy of i level which in this case is always equal to one.

The electronic spectra have been computed using the time-dependent density functional theory (TD-DFT), based on vertical excitations involving the three lowest-lying excited states.

RESULTS AND DISCUSSION

The optimized structure of the indigo molecule is shown in Figure 1, where we have indicated the atomic numbering

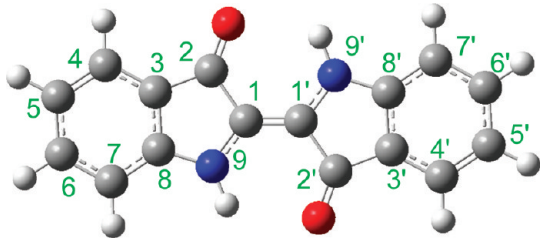

Figure 1. Indigo optimized structure.

scheme. The molecule is planar and symmetrical with respect to the central >C═C< double bond.

Indigo is a donor−acceptor molecule in which the amino groups act as the electron donors and the carbonyl groups as the electron acceptors. The intramolecular hydrogen bond between C═O and N−H groups keeps the molecule in a trans-planar configuration, blocking the trans−cis isomerization.[15]

Figure 2 shows the shape of the indigo HOMO and LUMO frontier orbitals. The red and green colors represent the positive and negative phases, respectively. It can be observed that both frontier orbitals show bonding and antibonding character. The HOMO is characterized by a long line of conjugated bonds that extends diagonally over the central carbon atoms, from C3′ to C3, with a contribution also from C7 and C7′. Carbons C6 and C6′ do not participate in the HOMO. These positions have a different reactivity than the rest of the molecule. In fact the introduction of substituents in the benzene ring has no pronounced effect in the color properties on the indigo dye. The C4−C5 and C4′-C5′ bond in the benzene ring, as well as the carbonyl and amino groups are antibonding with respect to the central carbon chain. In the LUMO π^* orbital several bonding and antibonding regions are observed. Carbons C5, C5′, C7, and C7′ are not involved, and the central C1 and C1′ carbons are antibonding.

$^\bullet$OH Initiated Oxidation of Indigo. In order to study the reactivity of indigo toward $\bullet OH$ radicals, we have considered

dx.doi.org/10.1021/jp211493k | J. Phys. Chem. A 2012, 116, 3643−3651

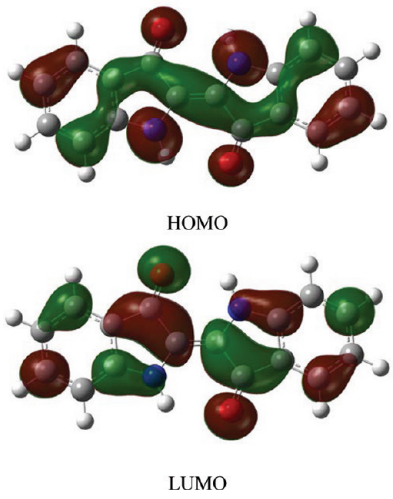

Figure 2. Frontier orbitals of the indigo molecule.

the H-abstraction from the NH site as well as all the •OH-addition pathways according to the following reactions

$$\text{indigo} + \bullet\text{OH} \rightarrow \text{indigo}(-\text{H})\bullet + \text{H}_2\text{O}$$

$$\text{indigo} + \bullet\text{OH} \rightarrow \text{indigo}(\text{OH})\bullet$$

Stationary points have been characterized on the potential energy surface of the reactions considered. In all cases the proposed complex mechanism has been used. Frequency calculations at 298.15 K on all of the stationary points were carried out at the same level of theory as the geometry optimizations to ascertain the nature of the stationary points.

H-Abstraction. Only hydrogen abstraction from amino groups has been considered, as it is well-known that abstraction of a hydrogen atom attached to a ring carbon atom is much less favored.

Equilibrium structures involved in the H-abstraction pathway have been identified and they are shown in Figure 3. Relative Gibbs free energies and relevant geometrical parameters are shown in the same figure, bond distances are given in Å.

In the prereactive (RC) complex, all of the atoms lie in the same plane (C_s molecular symmetry) and the •OH radical forms an eight member-ring structure with the central part of the indigo molecule (see Figure 3). Two hydrogen bonds are present. The strongest one corresponds to the interaction of the hydroxyl radical hydrogen atom with a lone pair of a carbonyl oxygen, at a distance of 1.858 Å; the other one is the interaction of the radical oxygen atom with an amino hydrogen, at a distance of 2.036 Å.

After the •OH free radical approaches the −NH group, the oxygen of •OH turns in the plane toward the hydrogen to be abstracted, as the energy increases to a maximum at the transition state. This is an early transition state, in which the amino hydrogen atom is 1.083 Å away from the N atom. According to the Hammond postulate, this kind of transition state corresponds to a fast exothermic reaction. A product complex is then obtained, which, in the next step, yields the final products, i. e., a water molecule and the corresponding radical, •Ind(-H). The product complex (PC) is shown in Figure 3. It can be seen that it also has C_s symmetry. In fact the whole reaction occurs in the molecular plane and the C_s symmetry is preserved throughout.

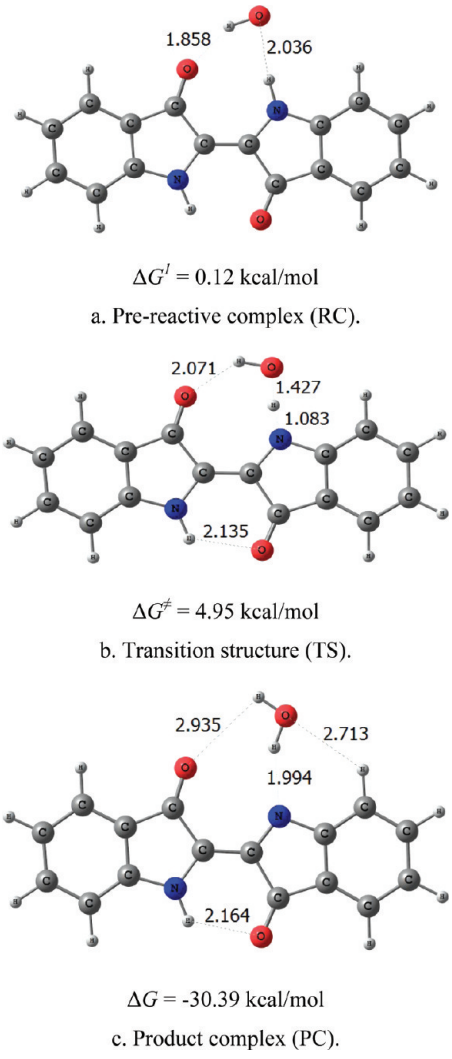

Figure 3. Stationary points in the H-abstraction by •OH radicals.

The final product is the •Indigo(-H) radical, which is shown in Figure 4a. It is very stable, its reaction free energy is less than −30 kcal/mol, probably due to the large delocalization of the formed radical unpaired electron that extends over the whole molecule. The radical spin density is represented in Figure 4b. Positive and negative spin densities are indicated in blue and green, respectively. Mulliken analysis spin density values are largest on C1 and N9′ atoms.

In addition, the SOMO of the radical resembles the HOMO of the indigo molecule, in that its conjugated system involves the same carbon atoms as in the free molecule (Figure 4c). This implies that the −NH hydrogen abstraction does not modify substantially the very large molecular conjugation which is at the basis of indigo stability. Conjugation is only broken at the C atom which is opposite to the abstraction site, i. e., when H is abstracted from N9′, the conjugation is broken at C8. In the figure, green and red regions correspond to positive and negative values of the orbital function.

Relative electronic energies (including ZPE) and Gibbs free energies (including thermodynamic corrections) are calculated with respect to the sum of the separated reactants, and they are reported in Table 1. In this table, ΔE_1 ($\Delta E_1 = E_{RC} - E_R$) is the prereactive complex stabilization energy, which also represents the barrier height for the unimolecular elementary reaction in

dx.doi.org/10.1021/jp211493k | J. Phys. Chem. A 2012, 116, 3643−3651

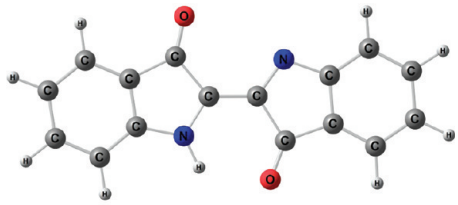

a. Structure of the •Indigo(-H) radical.

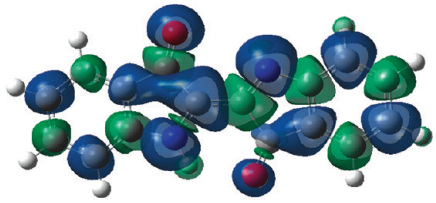

b. Spin density.

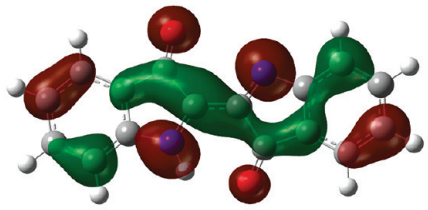

c. SOMO frontier orbital.

Figure 4. Structure (a), spin density (b), and SOMO frontier orbital (c) of the Indigo(-H)• radical.

Table 1. Relative Electronic Energies (Including ZPE) and Gibbs free energies (Including TCE), in kcal/mol, in the Amino H-Abstraction Reaction by an •OH Radical, at 298 K

path	ΔE_1	$\Delta E^{\ddagger}$	ΔE	ΔG_1	$\Delta G^{\ddagger}$	ΔG
H-abstraction	−7.96	−3.70	−28.64	0.12	4.95	−29.50

the first step of the complex mechanism. Analogously, $\Delta G_1 = G_{RC} - G_R$, is the prereactive complex stabilization Gibbs free energy. $\Delta E^{\ddagger}$ and $\Delta G^{\ddagger}$ are the energy and Gibbs free energy of the transition state relative to reactants, and ΔE and ΔG are the reaction energy and reaction Gibbs free energy.

The vibration mode corresponding to the imaginary frequency at the transition state indicates that this vibration is essentially the characteristic hydrogen atom motion between the NH hydrogen atom and the oxygen atom of the •OH radical. As the abstraction process involves an H atom displacement, it is associated with a significant imaginary frequency (-2722 cm^{-1}) which suggests that this elementary step presents a large transmission coefficient and could contribute significantly to the overall reaction rate.

•OH-Addition Channels. There are nine possible •OH-addition-type pathways that correspond to the radical oxygen atom binding to any carbon or N atom in the molecule. Given that the indigo molecule is planar, reaction from above or below the plane leads to equivalent products, and the symmetry number is 4 for all addition channels. The transition vector in the transition states structures corresponds to the vertical movement of the •OH group in the direction of the carbon or nitrogen sites. The hydrogen atom attached at the addition site folds back slightly to accommodate the incoming •OH radical. All additions occur in a similar way and modify the aromaticity of the indigo molecule because the C or N atom at the reaction site changes from an sp^2 to an sp^3 hybridization. As a result, adducts are not completely planar. However, only addition at C1 leads to a seriously bent molecule in which the two indol planes form an angle of 121.3 degrees.

The optimized geometries of the radical adducts in the •OH-addition pathways are presented in Figure 5, along with the most relevant nonbonding distances. Relative Gibbs free energies and relevant geometrical parameters are shown in the same Figure 5 (bond distances are given in Å). Cartesian coordinates of all transition structures are given in Table S1 of the Supporting Information.

The spin density and the SOMO frontier orbital of the C1 adduct radical are depicted in Figure 6. It can be seen that both the spin density and the SOMO molecular orbital of the C1 adduct are almost completely located on the molecular side opposite to the addition site.

Relative energies are calculated with respect to the sum of the separated reactants at 0 K, and they are reported in Table 2. In most cases, the reaction energy, ΔE, is negative, indicating that these reactions are energetically favored and irreversible and that their result depends on the stability of the formed adduct.

It is clear that addition on carbons at the central >C═C< double bond is, by far, the most favored addition channel, both in terms of barriers and of reaction energies and free energies. The preference for addition to C1 and C1′ is explained by the fact that these carbon atoms are the only ones that do not belong to an aromatic ring, Therefore, even if OH-addition suppresses the conjugation between both aromatic rings and dramatically changes the HOMO, it does not affect the aromaticity of the system, which involves the rings on each side. In agreement with this, the HOMO population on indigo is largest on the C1s. •OH-addition to C8 and N9 is endergonic and thus the corresponding formed adducts have not been represented in Figure 5. The electron pair on the nitrogen atom does not activate the addition to the C8 site.

Overall Indigo + •OH Reaction Channels. Two channels are clearly favored in this reaction: amino H-abstraction and addition to the central double bond. Both are expected to occur, as they have similar transition states free energy barriers (4.95 and 4.04 kcal/mol, for abstraction and addition, respectively) and their products are also about equally stable (by about 30 kcal/mol). Their free energy profiles are compared in Figure 7. One leads to the formation of the Indigo(-H)• radical, the other to the C1 •OH-adduct radical.

Branching ratios have been calculated at temperature T according to eq 1. Thus, the H-abstraction mechanism is calculated to account for about 18% of the •OH initiated oxidation, at 298 K.

UV−Vis Spectra. It is well-known that the intense coloring of organic molecules is due to the π conjugation system. The excitations that are responsible for the color of indigo present a $\pi-\pi^*$ character with a large oscillator strength. The reported λ_{max} corresponds to the transition energy from the ground electronic state to the first dipole-allowed excited state. Altering the π conjugation system of these compounds will result in changes in color or in decolorized products.

The indigo chromophore has been determined to involve the central atoms in the molecule, i.e. C1, C1′ and the carbonyl and the amino groups. It is of a donor−acceptor type, and the resulting color is very sensitive to the electron-donating-electron-accepting abilities of the component functional groups, while the benzene rings attached on either side have only a secondary influence on the color of the molecule.

dx.doi.org/10.1021/jp211493k | J. Phys. Chem. A 2012, 116, 3643−3651

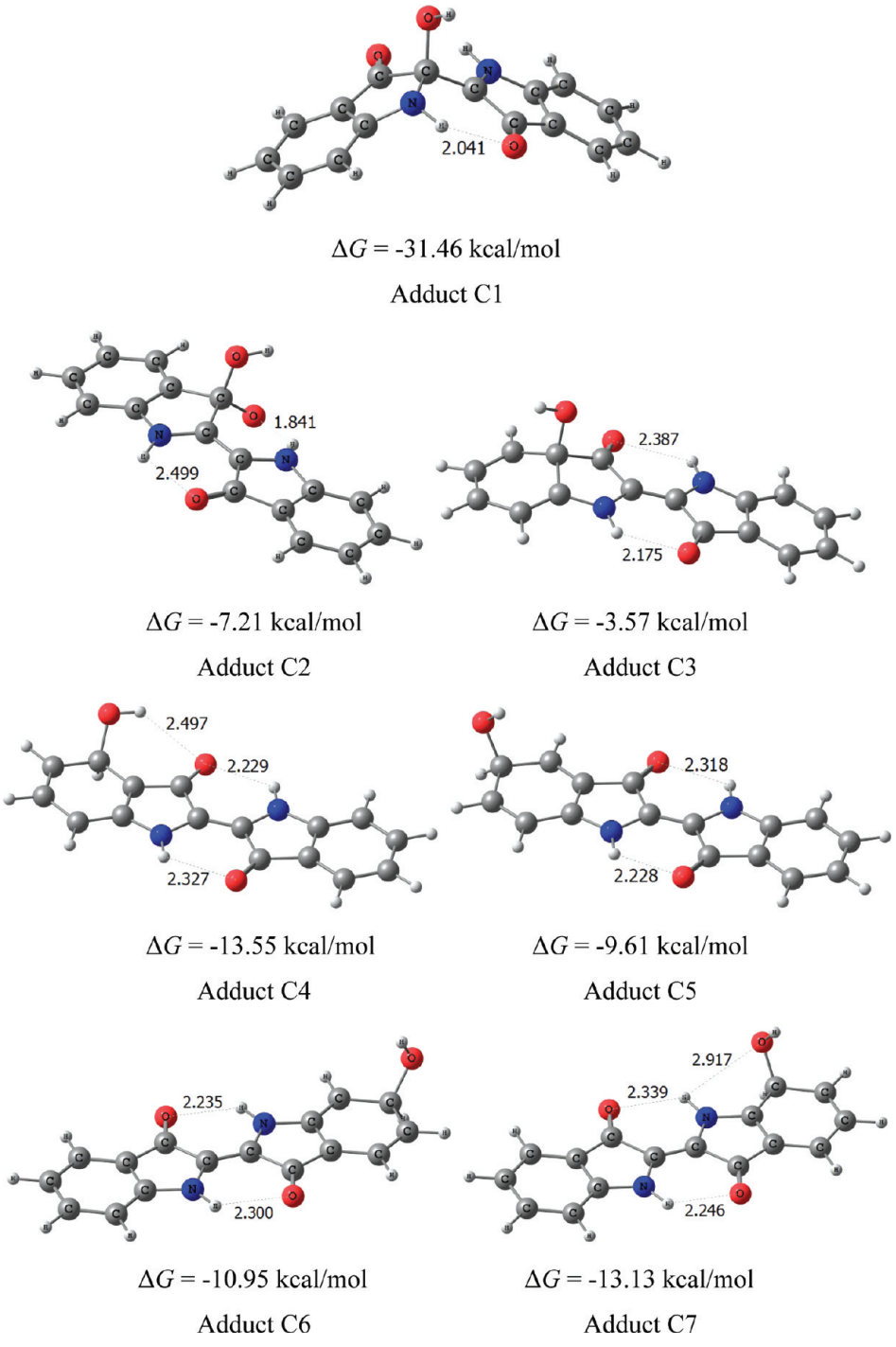

Figure 5. Adducts structures in the •OH-addition pathways.

We have computed the UV−vis spectra of indigo and of its major •OH degradation products: the dehydroindigo radical and the C1 adduct (Figure 8), using the time-dependent density functional theory (TD-DFT), based on vertical excitations involving the three lowest-lying excited states.

The computed UV−vis spectrum shows that the absorbance of the dehydroindigo radical, which accounts for about 18% of the reaction products in the first step of the OH reaction, is much smaller than the one for indigo, although the color shift is quite insignificant (λ_{max} shifts from 480 to 460 nm). On the other hand the C1 adduct is also less colored but red-shifted. However, these two radicals will rapidly (in a microsecond time scale) add O_2, and the resultant radicals will undergo further reactions. The main end product is isatin, in both cases. Its UV/vis spectrum is also shown in Figure 8. Thus, the formation of the major products considerably modifies the spectrum while partially preserving the same color. This could explain the fading of indigo in contact with reactive oxygen species (ROS).

•OOH Initiated Oxidation of Indigo. In order to study the reactivity of indigo toward atmospheric peroxyl radicals, we have considered the smallest of them, the •OOH radical. Following a procedure similar to that described in the case of

dx.doi.org/10.1021/jp211493k | J. Phys. Chem. A 2012, 116, 3643−3651

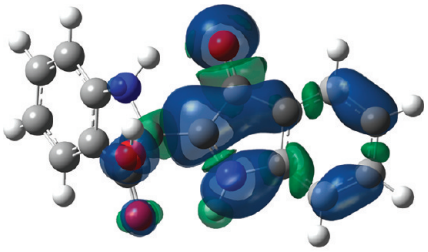

a. Spin density.

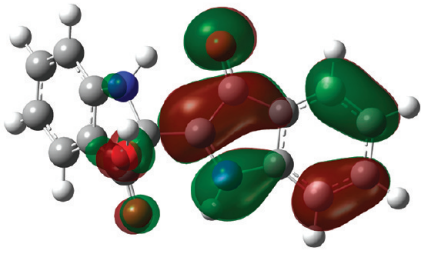

b. SOMO frontier orbital.

Figure 6. Spin density (a) and SOMO frontier orbital (b) of the C1 adduct radical.

Table 2. Relative Electronic Energies (Including ZPE) and Gibbs Free Energies (Including TCE at 298 K), in kcal/mol, in the •OH-Addition Pathways, in the Gas Phase

OH-addition	$\Delta E^{\ddagger}$	ΔE	$\Delta G^{\ddagger}$	ΔG
C1	−4.65	−40.42	4.04	−31.46
C2	1.10	−16.23	6.00	−7.21
C3	0.17	−12.67	9.12	−3.57
C4	1.39	−22.29	9.45	−13.55
C5	−0.31	−18.20	8.05	−9.61
C6	2.07	−19.63	10.36	−10.95
C7	−1.24	−21.79	7.29	−13.13
C8	2.93	2.41	11.71	11.78
N9	14.19	4.54	23.64	14.34

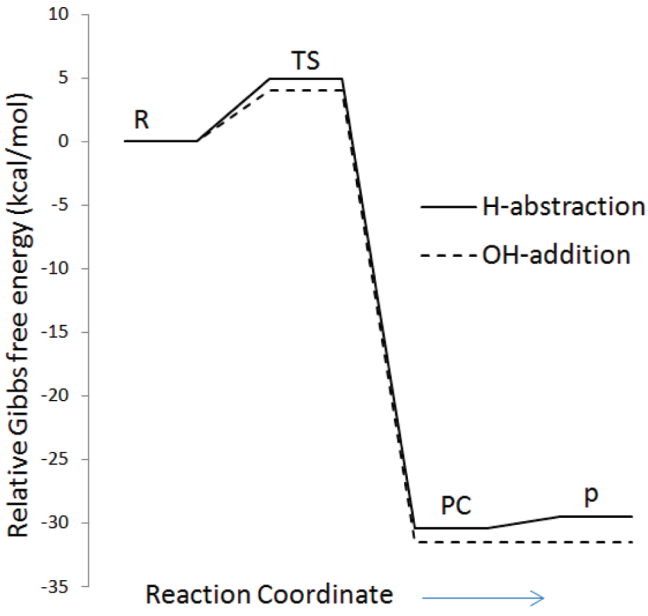

Figure 7. Relative Gibbs free energy profiles of the H-abstraction and C1 •OH-addition channels.

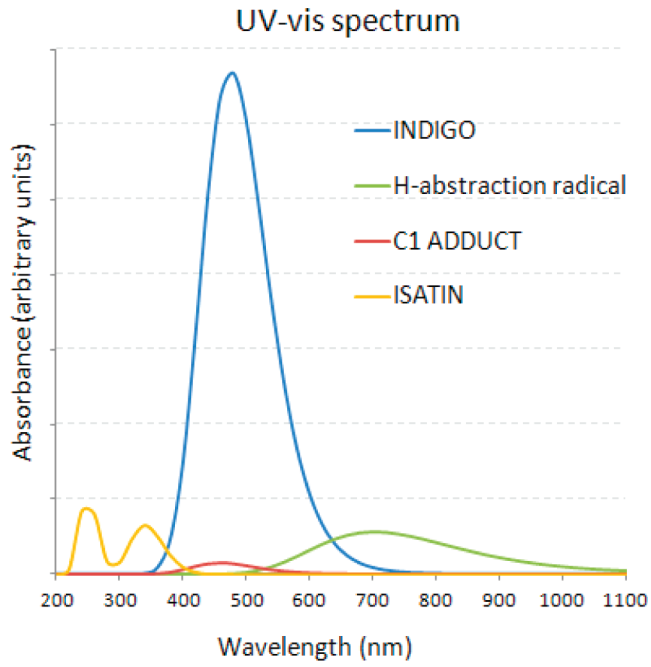

Figure 8. Computed UV−vis spectrum of indigo, the H-abstraction radical, the C1 adduct, and isatin.

•OH radical reactions, we have considered all possible H-abstraction and •OOH-addition pathways, according to

$$\text{indigo} + \bullet\text{OOH} \rightarrow \text{indigo}(-\text{H})\bullet + \text{H}_2\text{O}_2$$

$$\text{indigo} + \bullet\text{OOH} \rightarrow \text{indigo}(\text{OOH})\bullet$$

The thermochemical feasibility of the different mechanisms and reaction channels was investigated first, since it determines the viability of chemical processes. •OOH additions proceed by binding the terminal oxygen atom to a carbon atom. In addition we have considered a complex mechanism similar to the one first proposed by Anglada and Domingo[33,34] for the gas-phase reaction between formaldehyde and a hydroperoxyl radical. The electronic features of this reaction mechanism have been discussed, and the process was described as a proton-coupled electron-transfer (PCET). In the case of formaldehyde, it is exothermic by 16.8 kcal/mol and the calculated rate constant at 300 K is 9.29×10^{-14} cm^3 molecule^{-1} s^{-1}. Following this example, we have studied the concerted addition of •OOH to the carbonyl group of an indigo molecule. It involves the transfer of a proton from the hydroperoxyl moiety to the oxygen of the indigo carbonyl group, the simultaneous addition of the terminal oxygen to the carbonyl carbon, and an intermolecular electron transfer between the two •OOH oxygen atoms. Although the energy barrier is negative, the process is calculated to be endergonic in terms of Gibbs free energy. In addition we have investigated a similar mechanism for the •OOH addition to the central double bond, but again the reaction is endergonic.

The relative energies (ΔE) and Gibbs free energies of reaction (ΔG) for all of the studied channels are reported in Table 3. Results for the above concerted mechanisms are indicated as >C═O and >C═C<.

Results are very different than the ones obtained with the •OH radical, the difference in reactivity being related to the electron-accepting character of the reacting radical. As can be seen from Table 3, most reactions are endergonic. Only the

dx.doi.org/10.1021/jp211493k | J. Phys. Chem. A 2012, 116, 3643−3651

Table 3. Relative Reaction Energies (Including ZPE) and Reaction Gibbs Free Energies (Including TCE at 298 K), in kcal mol^{-1}, in the Indigo + •OOH Pathways, in the Gas Phase

path	ΔE	ΔG
	H-Abstraction	
N9	3.29	3.24
	•OOH-Addition	
C1	−13.47	−1.92
C2	17.53	29.18
C3	13.11	24.54
C4	2.89	13.67
C5	7.42	18.08
C6	5.99	16.86
C7	4.45	15.09
C8	9.77	20.84
N9	14.90	25.00
>C═O<	−3.00	8.71
>C═C<	−2.69	9.17

•OOH addition to the C1 and C1′ central double bond carbons is feasible, and it is computed to be exergonic by 1.92 kcal/mol (see Table 3). The result of hydrogen abstraction by •OOH is the formation of a radical plus H_2O_2, but this reaction is computed to be endergonic (3.24 kcal/mol; see Table 3).

Endergonic reaction channels will not be considered in this work. Even if they take place at a significant rate, they would be reversible, and therefore, the formed products would not be observed. Addition channels might, in principle, be significant if their products rapidly react further and if no fast parallel reactions occur. This would be particularly important if these later stages were sufficiently exergonic to provide a driving force, and if their reaction barriers were low. This is not the case here. Thus, in the following discussion, only the C1 addition pathway will be studied in detail.

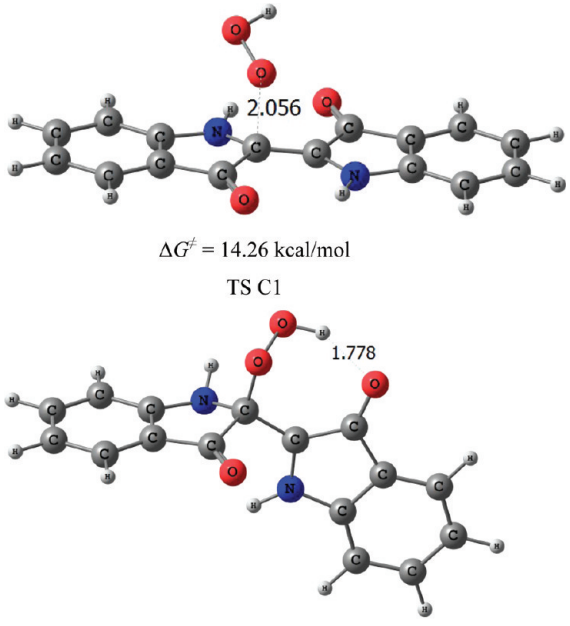

Figure 9. Stationary structures in the •OOH addition to C1.

The transition state (TS C1) and an adduct complex (PC C1) have been obtained for the C1 addition pathway, as shown in Figure 9. Relative Gibbs free energies and relevant geometrical parameters are shown on the same figure (bond distances are given in Å). In the C1 transition state structure, the peroxyl radical is approximately perpendicular to the molecular plane. The transition vector in the transition state corresponds to the vertical movement of the •OOH group in the direction of the carbon site. In the C1 adduct structure, the external O atom of the •OOH radical binds to the central >C═C< double bond of the indigo molecule, and the H atom of the •OOH radical forms a hydrogen bond with the indigo ═O atom. It is possible that the next step in the reaction could be the formation of an •OH radical. A hydrogen bond is observed between the •OOH hydrogen atom and the indigo carboxyl oxygen atom on the opposite side. Cartesian coordinates of the C1 transition structure and C1 adduct are given in Table S2 of the Supporting Information.

The free energy barrier for the •OOH radical addition to C1 is 14.26 kcal/mol, which is considerably higher than the one for the •OH radical addition (4.95 kcal/mol). However, even if the •OOH concentration is considerably larger than the one of the hydroxyl radical, these reactions are not expected to contribute to indigo oxidation under atmospheric oxidative conditions.

The spin density and the SOMO molecular orbital of the •OOH C1 adduct are represented in Figure 10. Both are almost completely located on the molecular side opposite to the addition site.

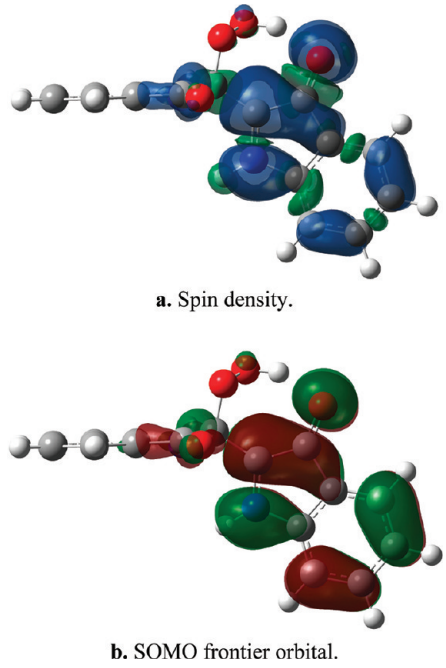

a. Spin density.

b. SOMO frontier orbital.

Figure 10. Spin density (a) and SOMO frontier orbital (b) of the •OOH C1 adduct radical.

CONCLUSIONS

In this work, we have carried out a detailed mechanistic quantum chemistry study on the reactivity of the indigo dye toward hydroxyl (•OH) and hydroperoxyl (•OOH) radicals under atmospheric oxidative conditions. All reaction pathways have been investigated, and all stationary points have been

dx.doi.org/10.1021/jp211493k | J. Phys. Chem. A 2012, 116, 3643−3651

characterized on the potential energy surface of the considered reactions. Electronic and Gibbs free energies relative to the separated reactants have been reported.

On the basis of the calculated Gibbs free energies, we conclude that the reaction between the indigo molecule and the hydroxyl radical occurs mainly through two different mechanisms: H-abstraction from an NH site and •OH-addition to the central double bond. •OH-addition is the main reaction channel, while H-abstraction accounts for about 18% of the total reaction. Unfortunately, branching ratios depend a little on the particular quantum chemistry method that is used. However, it is generally assumed that the uncertainty in the free energy barriers for •OH abstraction and addition calculated with the M05-2X functional[20] is about 1 kcal/mol. More important is the fact that trends usually are the same in all accurate methods. Since the meaningful energy differences are quite large, our conclusions can be safely assumed to be correct. In both reactions, the structure of the indigo chromophore group is modified, and thus the color is changed. This mechanism adequately accounts for the loss of chromophore in urban air, including indoor air such as in museums and in urban areas.

Regarding the reactivity of indigo toward •OOH radicals, we have found that only •OOH-addition to the central bond is feasible. All other channels present positive reaction Gibbs free energy values. However, the free energy barriers are considerably higher than in the case of the •OH radical addition, the difference in reactivity between •OH and •OOH radicals being directly related to their electron-accepting character. Even if the •OOH concentration is usually about a hundred times larger than the one of •OH radicals, this reaction is not expected to contribute significantly to indigo oxidation.

■ ASSOCIATED CONTENT

Supporting Information

Cartesian coordinates of the transition structures in the •OH radical addition pathways (Table S1) and Cartesian coordinates of the transition structure and adduct in the •OOH radical addition to C1 (Table S2). This material is available free of charge via the Internet at http://pubs.acs.org.

■ AUTHOR INFORMATION

Corresponding Author

*E-mail: ciuga@xanum.uam.mx.

Notes

The authors declare no competing financial interest.

■ ACKNOWLEDGMENTS

This work is a result of the FONCICYT Mexico-EU 'RMAYS' network, Project No. 94666 and CONACYT Project 153663 CB-2010-01. We gratefully acknowledge the computer time from Laboratorio de Visualización y Cómputo Paralelo at Universidad Autónoma Metropolitana-Iztapalapa and Dirección General de Cómputo y de Tecnologías de Información y Comunicación (DGCTIC) at Universidad Nacional Autónoma de México. Cristina Iuga thanks CONACYT for Fellowship No. 148744 (Apoyos Complementarios para la Consolidación Institucional de Grupos de Investigación).

■ REFERENCES

(1) Deganoa, I.; Biesagab, M.; Colombinia, M. P.; Trojanowiczb, M. *J. Chromatogr. A* **2011**, *1218*, 5837.
(2) Poulin, J. *J. Can. Assoc. Conserv.* **2007**, *32*, 48−56.
(3) Griffiths, J. In *Developments in the Chemistry and Technology of Organic Dyes*, Griffiths, J., Ed.; Blackwell: London, 1984.
(4) Grosjean, D.; Sensharma, D. K.; Cass, G. R. *Sci. Total Environ.* **1994**, *152*, 125.
(5) Grosjean, D.; Grosjean, E.; Williams, E. L. *Sci. Total Environ.* **1994**, *151*, 213.
(6) Grosjean, D.; Grosjean, E.; Whitmore, P. M.; Cass, G. R.; Druzik, J. R. *Environ. Sci. Technol.* **1988**, *22*, 292.
(7) Novotna, P.; Boon, J. J.; van der Horst, J.; Pacakova, V. *Color. Technol.* **2003**, *119*, 121.
(8) Vine, K. L.; Matesic, L.; Locke, J. M.; Ranson, M.; Skropeta, D. *Anti-Cancer Agents Med. Chem.* **2009**, *9*, 397.
(9) Mock, G. N.; Rucker, J. W. *Am. Dyestuff Rep.* **1991**, *80*, 15.
(10) Reidies, A. H.; Jensen, D.; Guisti, M. *Textile Chem. Color.* **1992**, *24*, 26.
(11) Iuga, C.; Solís-Correa, H.; Ortíz, E. *Proc. 2011 NSTI-Nanotech Conf.* **2011**, *3*, 624.
(12) Dusanter, S.; Vimal1, D.; Stevens, P. S.; Volkamer, R.; Molina, L. T. *Atmos. Chem. Phys.* **2009**, *9*, 1665.
(13) Hermans, I.; Müller, J. F.; Nguyen, T. L.; Jacobs, P. A.; Peeters, J. *J. Phys. Chem. A* **2005**, *109*, 4303.
(14) Solís Correa, H.; Ortiz, E.; Uc, V. H.; Barceló Quintal, I. D.; Hernández Avila, J. L. *Mol. Simul.* **2011**, *37*, 1085.
(15) Yamazaki, S; Sobolewski, A. J.; Domcke, W. *Phys. Chem. Chem. Phys.* **2011**, *13*, 1618.
(16) Frisch, M. J.; Trucks, G. W.; Schlegel, H. B.; Scuseria, G. E.; Robb, M. A.; Cheeseman, J. R.; Scalmani, G.; Barone, V.; Mennucci, B.; Petersson, G. A.; Nakatsuji, H.; Caricato, M.; Li, X.; Hratchian, H. P.; Izmaylov, A. F.; Bloino, J.; Zheng, G.; Sonnenberg, J. L.; Hada, M.; Ehara, M.; Toyota, K.; Fukuda, R.; Hasegawa, J.; Ishida, M.; Nakajima, T.; Honda, Y.; Kitao, O.; Nakai, H.; Vreven, T.; Montgomery Jr., J. A.; Peralta, J. E.; Ogliaro, F.; Bearpark, M.; Heyd, J. J.; Brothers, E.; Kudin, K. N.; Staroverov, V. N.; Kobayashi, R.; Normand, J.; Raghavachari, K.; Rendell, A.; Burant, J. C.; Iyengar, S. S.; Tomasi, J.; Cossi, M.; Rega, N.; Millam, J. M.; Klene, M.; Knox, J. E.; Cross, J. B.; Bakken, V.; Adamo, C.; Jaramillo, J.; Gomperts, R.; Stratmann, R. E.; Yazyev, O.; Austin, A. J.; Cammi, R.; Pomelli, C.; Ochterski, J. W.; Martin, R. L.; Morokuma, K.; Zakrzewski, V. G.; Voth, G. A.; Salvador, P.; Dannenberg, J. J.; Dapprich, S.; Daniels, A. D.; Farkas, O.; Foresman, J. B.; Ortiz, J. V.; Cioslowski, J.; Fox, D. J. *Gaussian 09*, revision A.02; Gaussian, Inc.: Wallingford, CT, 2009.
(17) Zhao, Y.; Schultz, N. E.; Truhlar, D. G. *J. Chem. Theory Comput.* **2006**, *2*, 364.
(18) Zavala-Oseguera, C.; Alvarez-Idaboy, J. R.; Merino, G.; Galano, A. *J. Phys. Chem. A* **2009**, *113*, 13913.
(19) Velez, E.; Quijano, J.; Notario, R.; Pabón, E.; Murillo, J.; Leal, J.; Zapata, E.; Alarcón, G. *J. Phys. Org. Chem.* **2009**, *22*, 971.
(20) Vega-Rodriguez, A.; Alvarez-Idaboy, J. R. *Phys. Chem. Chem. Phys.* **2009**, *11*, 7649.
(21) Galano, A.; Francisco-Marquez, M.; Alvarez-Idaboy, J. R. *Phys. Chem. Chem. Phys.* **2011**, *13*, 11199.
(22) Galano, A.; Alvarez-Idaboy, J. R. *Org. Lett.* **2009**, *11*, 5114.
(23) Perez-Gonzalez, A.; Galano, A. *J. Phys. Chem. B* **2011**, *115*, 1306.
(24) Leon-Carmona, J. R.; Galano, A. *J. Phys. Chem. B* **2011**, *115*, 4538.
(25) Galano, A. *Phys. Chem. Chem. Phys.* **2011**, *13*, 7147.
(26) Black, G.; Simmie, J. M. *J. Comput. Chem.* **2010**, *31*, 1236.
(27) Furuncuoglu, T.; Ugur, I.; Degirmenci, I.; Aviyente, V. *Macromolecules* **2010**, *43*, 1823.
(28) Galano, A.; Macías-Ruvalcaba, N. A.; Campos, O. N. M.; Pedraza-Chaverri, J. *J. Phys. Chem. B* **2010**, *114*, 6625.
(29) Gao, T.; Andino, J. M.; Alvarez-Idaboy, J. R. *Phys. Chem. Chem. Phys.* **2010**, *12*, 9830.
(30) Iuga, C.; Sainz-Díaz, C. I.; Vivier-Bunge, A. *Geochim. Cosmochim. Acta* **2010**, *74*, 3587.

(31) Iuga, C.; Alvarez-Idaboy, J. R.; Vivier-Bunge, A. *J. Phys. Chem. A* **2011**, *115*, 5138.
(32) (a) Alvarez-Idaboy, J. R.; Mora-Diez, N.; Vivier-Bunge, A. *J. Am. Chem. Soc.* **2000**, *122*, 3715. (b) Alvarez-Idaboy, J. R.; Mora-Diez, N.; Boyd, R. J.; Vivier-Bunge, A. *J. Am. Chem. Soc.* **2001**, *123*, 2018. (c) Uc, V. H.; Alvarez-Idaboy, J. R.; Galano, A.; Vivier-Bunge, A. *J. Phys. Chem. A* **2006**, *110*, 10155. (d) Francisco-Marquez, M.; Alvarez-Idaboy, J. R.; Galano, A.; Vivier-Bunge, A. *Phys. Chem. Chem. Phys.* **2003**, *5*, 1392. (e) Iuga, C.; Alvarez-Idaboy, J. R.; Vivier-Bunge, A. *Theor. Chem. Acc.* **2011**, *129*, 209. (f) Iuga, C.; Alvarez-Idaboy, J. R.; Reyes, L.; Vivier-Bunge, A. *J. Phys. Chem. Lett.* **2010**, *1*, 3112.
(33) Olivella, S.; Anglada, J. M.; Sole, A.; Bofill, J. M. *Chem.—Eur. J.* **2004**, *10*, 3404.
(34) Anglada, J. M.; Domingo, V. M. *J. Phys. Chem. A* **2005**, *109*, 10786.